Enhancement Wear Properties of HSS-M2 Tool Steel with WC Deposited by SMAW Process

D. Najafipour [1] , I. Ebrahimzadeh [*2]

Advanced Materials Research Center, Department of Materials Engineering, Najafabad Branch, Islamic Azad University

Abstract

In this study, the effect of cladded tungsten carbide layer upon HSS-M2 tool steel on microstructure, hardness, and wear behavior has been studied in two cases without using the middle layer and with using the middle layer of nickel. Tungsten Carbide cladded on HSS-M2 tool steel by Arc Weld (SMAW). The ASTM-G65 wear test was used to determine its application in mineral industry. The results showed that the formation of M_6C (tungsten-rich carbide) on deposited layer, as well as tungsten carbide with the formation of a composite layer on the base metal surface, increased the wear resistance up to 60% and the hardness up to 150% compared to the uncoated sample. Comparing the results in terms of the use or non-use of the middle nickel layer indicates the improvement of wear behavior without using middle nickel layers.

*Keywords***:** Hard facing; HSS Steel; SMAW process; WC cladding; Wear behavior.

1. Introduction

The repair and restore of cutting tools have a decisive role in increasing their service life and productivity, therefore the maintenance issue is directly concerned with industries involved mining although the cold work tool steel due to high carbon content and alloying elements have poor weldability, many attempts were done to apply hard coatings to increase their wear behavior. Strengthen the surface by a hard phase can be the best alternative to improve the wear resistance in soft materials without an effective change in the properties such as density. This partial improvement depends on the parameters of the enhancer phase such as (size, geometric shape and hardness) and inherent properties such as hardness, plasticity and bonding properties between the second phase and the base metal [1)]. Fishman et.al. used laser process on tool steel M2, injected tungsten carbide powder directly into the molten pool. The hardness observed in the 1100-1200 HV range was for coatings with 40 to 50 percent tungsten and up to 1600 HV in the upper layer with 75 % weight of tungsten [2)]. Lane applied Multi-layer welding with tungsten carbide powder on medium carbon steel AISI1050 by GTAW process. The evaluation of the microstructure and wear performance of the sample formed a vein-like phase, Fe_3W_3C, showed that the hardness and wear behavior of the coated layers increased [3)]. Bechley et.al. developed three different coatings on the steel substrate by SMAW process. The best wear resistance observed in the sample with the microstructure of

* *Corresponding author*
Tel: +98 9132387095
E-mail: i.ebrahimzadeh@pmt.iaun.ac.ir
Address: Advanced Materials Research Center, Department of Materials Engineering, Najafabad Branch, Islamic Azad University, Najafabad, Iran
1. M.Sc.
2. Assistant professor

eutectic and M_7C_3 carbides. The main wear mechanism is observed as a micro-cutting abrasion and fracture of carbides [4]. Niosef et.al. found that adding 20 wt.% of tungsten carbide powder to HSS-M2 steel, caused an increase in M6C carbide. These carbides showed a multi-model size distribution that composed of ~5.9 μm eutectic carbide along the grain boundary and ~0.25 μm of carbide distributed inside the grains. Also, more quantities of quasi-stable austenite (~88 % Vol), were seen that the high wear resistance of these coatings was determined by $y \rightarrow \alpha$ forming a hard metal material and a multi-model size distribution [5]. Wang et.al. coated tungsten carbide and titanium carbide powders on low carbon steel by the GTAW process. The sample coating with tungsten carbide powder containing titanium metal powder had the best wear performance in all the other samples that cladded by tungsten carbide. Also, under low-speed slip conditions, all types of TiC and TiC+WC coatings had a better wear performance than other coatings [6]. Bonk et.al. used the laser welding to deposit WC, VC, TiC, SiC, Si_3N_4 and Al_2O_3 on HSS (HS6-5-3-8). Adding these particles caused reducing the size of dendrites in the microstructure, and integration of the surface layer occured by enriching the surface layer of alloying supplements derived from alloying elements [7]. Vakius et.al. concluded that the alloy was uniformly concentrated on the surface of a soft material. Welding increased hardness and wear resistance without diminishing the ductility and toughens properties of the created layer. wide variety of surface hardening alloys are available for keeping anti-wear property, and dispersion of carbides in the matrix of the austenite [8]. Otunnello et.al. investigated the welding parameters of tungsten carbide and divided tungsten carbides into two mono-carbide and di-carbide. Also, a molten eutectic carbide containing mono-carbide plus di-carbide that is one of the toughest anti-wear materials used in modern anti-wear technology [9]. Hashemi et.al. investigated the wear behavior of different carbides coatings of V, Mo, W on the HSS tool steel and with a pin and disk wear test found that vanadium-rich carbides had a better wear behavior than W carbide [10]. Foumin et.al. examined microstructure parameters, hardness and wear resistance of tungsten carbide, nickel-chrome, and iron powder. The results showed that by creating binary structures and orbing tungsten carbide particles, spheres and triple wear resistance compared to tool steel were obtained [11]. Hubner et al. examined the tungsten carbide coating on Inconel 625 with different weight percentages, wear behavior and hardness, as well as they found adding more than 30% weight of tungsten carbide with forming strong hydroxide formation around the grains led to an increase in hardness [12].

However, a wide range of researches in this field of applying tungsten carbide coating on tool steels, especially the widely used HSS-M2 tool have not been investigated by the available and widely used SMAW method. Considering that the parts are generally needed in the mining industry in the restoration of the workplace, it is not possible to apply laser processes, thermal sprays and TIG welding for them. In this research, the effect of applying tungsten carbide coating by the SMAW method in two conditions of the presence and the absence of an intermediate layer has been investigated. Nickel as an interlayer used to improve the toughness and wear resistance of the interface and to enhance the connection of base metal and welding metal.

2. Materials and Methods

In this study, HSS-M2 steel with the percentage of the elements specified in Table 1 was used as the base metal. For coating, the tungsten carbide electrode (OKs 448 ELK) and also the nickel electrode as an intermediate layer used with an analysis that is presented in Table 2.

Table 1. Chemical composition of tool steel base metal (HSS-M2).

Fe	C	Si	Cr	Mo	Ni	Co	V	W	Mn
Rem	0.7	0.4	4.5	4.5	0.073	0.106	2	6	0.345

Table 2. Chemical composition of electrode used in this research.

Element (wt. %)	Fe	Ni	W_2C	Mn	Si
Electrode ELK Oks448	39.5	-	58	1.3	1.2
Nickel electrode Ok Ni-1	-	100	-	-	-

Five samples with dimensions of 101×25×5 mm were cut using wire cut without applying the tungsten layer. The samples were free of any oxide or grease film through the wire brush. Before starting welding with regard to carbon percentage equivalent to the base metal (2.054) each sample preheated up to 300 °C (AWS D1.1-96 ANNEX XI). Sample codes required for this study and used in Eq. 1 to the required parameters determined in Table 3.

The equivalent carbon is obtained from Eq. (1).

$$Ce= C+Mn/6+(Cr+Mo+V)/5+(Ni+Cu)/15 \quad \text{Eq. (1)}$$

Then the samples were broken down again through wire cut to the dimensions of76×25×5 mm for placing in wear test device with the standard ASTM G65 [13] that is shown in Fig. 1. The structure of the coated samples in the coated area and the interface of base metal and the coated area were evaluated through optical microscopy and scanning electron microscopy (TESCAN- XMU). Also, EDS analysis was used to investigate the sediment.

Table 3. Nomenclature of the test specimens, type, pass numbers, and interlayer status.

Raw	Base metal type	Used inter layer Ni	Number of applied passes WC
1	HM2	Doesn't have	Doesn't have
2	HM2-1-Ni	Has	One layer
3	HM2-2-Ni	Has	Two-layer
4	HM2-1	Doesn't have	One layer
5	HM2-2	Doesn't have	Two-layer

Considering that the purpose of this coating is to increase the efficiency of M2 steel in the mining industry an accurate examination of wear resistance of the coated layer and the wear resistance test of base steel were conducted based on ASTM G65 standard. Dimensions of samples are according to the 76×25×5 mm standard. With regard to the high hardness of the samples, a method in the standard was used. The time required for each sample was 30 minutes and applied weight for each sample was 150 N. The parameters selected in accordance with the standard including the rate of sand (300 to 400 g/min) and the speed (200 ± 10 round per minute). The samples were weighed before and after the test using a digital scale with precision of 0.001 gr, and, by using Eq. (2), the lost volume of each sample was obtained [7].

$$V=m/\rho \times 1000 \quad \text{Eq. (2)}$$

which in V is the lost volume (mm^3), m is the weight difference before and after the test (g), ρ is the density (g/cm^3).

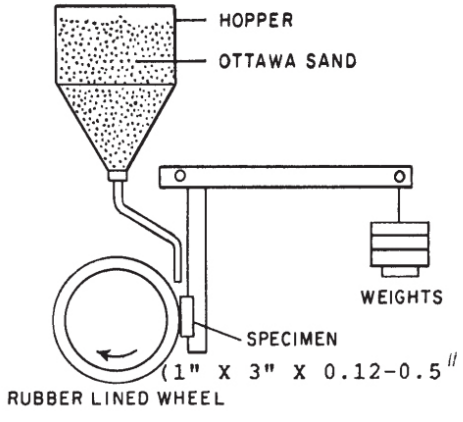

Fig. 1. Schematic of wear test device related to standard ASTM-G65 [13].

3. Results and Discussion

3. 1. Microstructural evaluation

The microstructure derived from the base metal of the HM2 sample (base metal) is shown in Fig. 2. The microstructure consists of remaining austenite in the plate martensite. Due to the high carbon content (2.054) and hypereutectoid composition, the structure of the base metal is plate martensite. In this Sample, because no welding process has been performed, due to the production of base metal, freezing time is low, so the retained austenite in the matrix of martensite was observed.

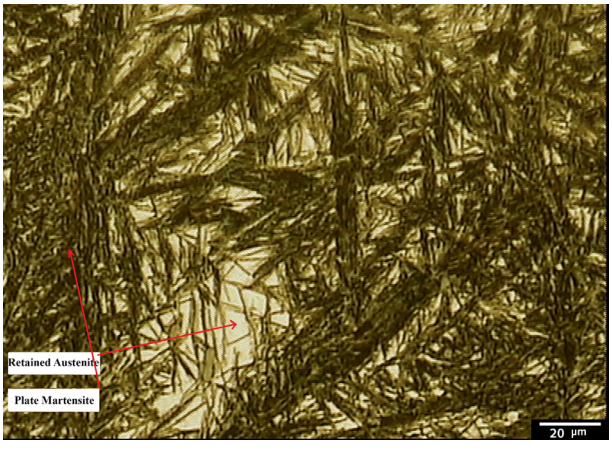

Fig. 2. The microstructure of base metal HM2 used in this research.

Fig 3 A-D shows the microscopic structure of the heat-affected zone in HM2-1, HM2-2, HM2-1Ni, HM2-2Ni samples respectively. The resulting microstructure, with regard to the welding heat, was coarsened and Ultimately caused a large change in the mechanical properties in which the most important one increasing in hardness.

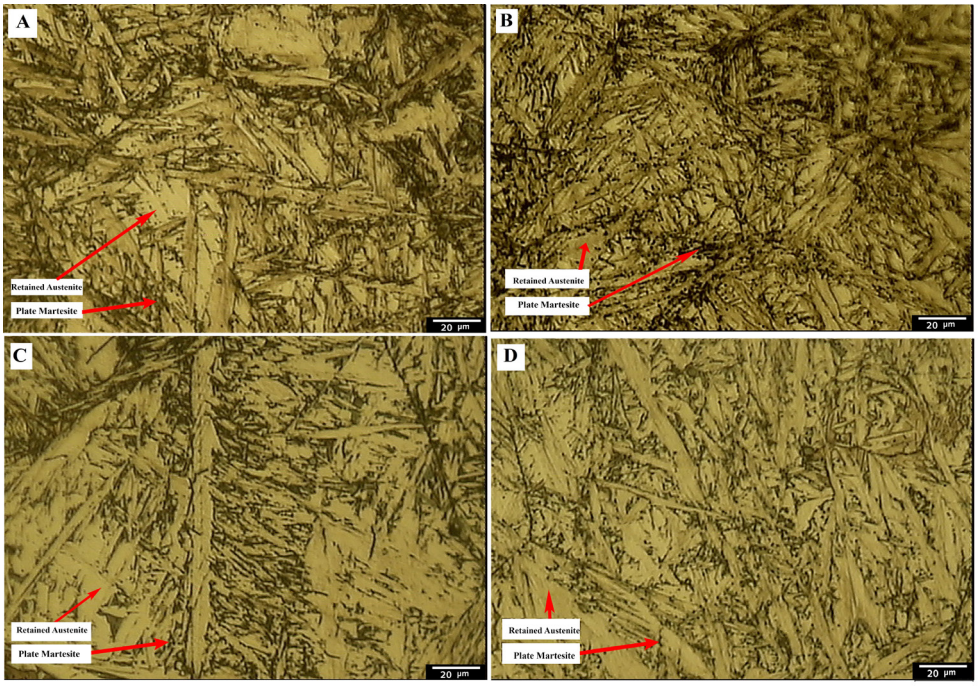

Fig. 3. The microscopic structure of the heat- affected zone by the welding in A- HM2-1, B-HM2-2, C-HM2-1Ni, D-HM2-2Ni samples.

Fig. 4 shows the microstructure of the middle layer pure nickel that was used only in samples with HM2-2-Ni and HM2-1-Ni codes. To improve the toughness and wear resistance of the interface and improve the connection of base metal and welding metal, the middle layer of nickel was used. The microstructure consists of solid solution of nickel. Nickel as an interlayer used to improve the toughness and wear resistance of the interface and to enhance the connection of base metal and welding metal.

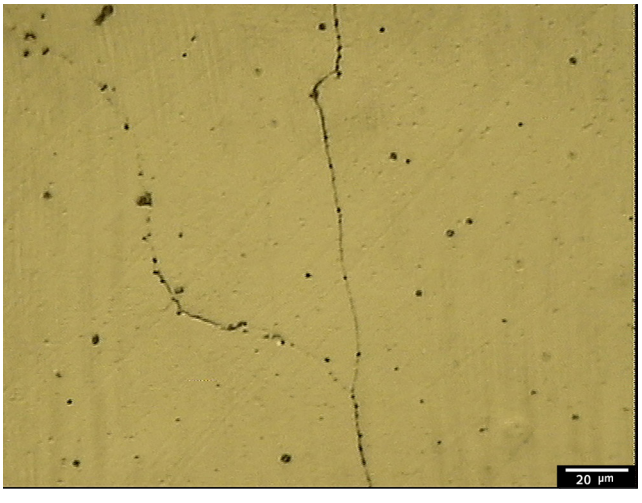

Fig. 4. The microstructure of the middle layer nickel used in samples of HM2-1-Ni and HM2-2-Ni.

Fig. 5 shows the microstructure of the welding region in the samples with the codes specified in Table 3, which includes the distribution of carbide in the matrix of α. During solidification, tungsten precipitates as carbide and formed a flake and around ones in the matrix of low carbon and ferrite-like structures. However, the only difference in Fig. 5A to D is the type of growth of their grains at the solidification zone. Two important and effective parameters in the formation of grains include the rate of cooling and the alloying elements. Since the temperature gradient is the same in the samples in condition of without interlayer of Nickel and with interlayer

of Nickel, the only difference between these two forms is the nickel penetration into the weld structure. The nickel crystal lattice is FCC and at the ambient temperature, does not have solubility in the base metal and the weld metal with crystal lattice of BCC. This phenomenon caused a pushing back in front of the frozen section. The progression of freezing and frozen section movement forward led to the formation of dendritic arms [15].

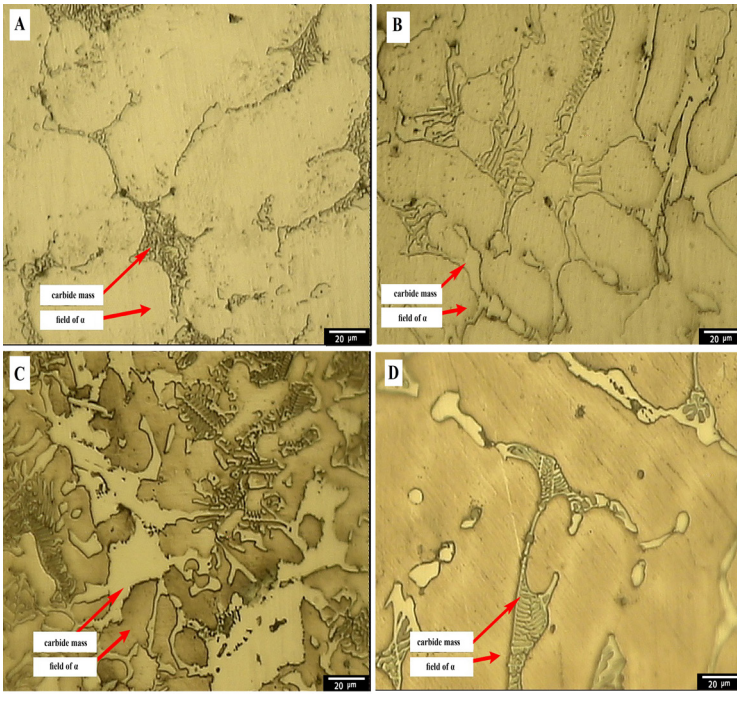

Fig. 5. The microscopic structure of the welded zone by the welding in A-HM2-1,B-HM2-2, C-HM2-1Ni, D-HM2-2Ni samples.

Fig. 6 consists of the microstructure analysis of the interface between the base metal, the middle layer, and the welded metal. Fig. 6-A is in the mode of using the nickel intermediate layer and the Fig. 6.B does not use the nickel intermediate layer. In conditions A: using the nickel middle layer and B: without using the middle layer.

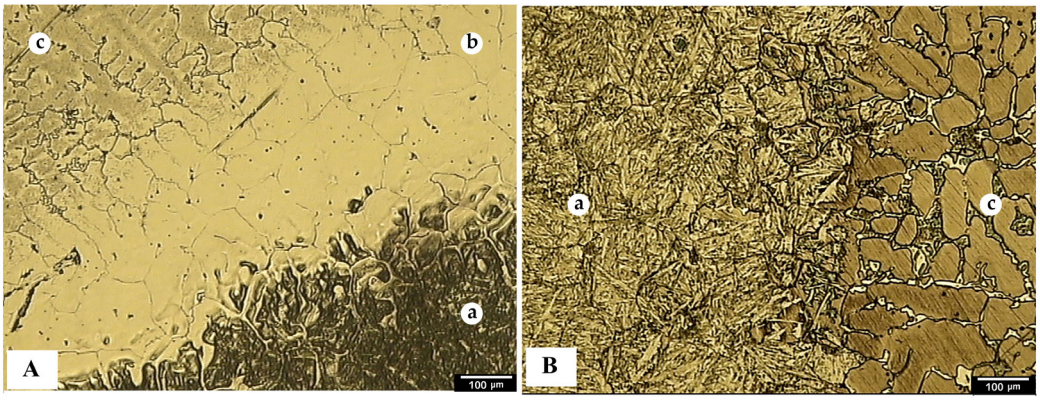

Fig. 6-A Microstructure of the interface between (a-base metal) and (b- middle layer) and (c-weld metal) and B- Microstructure of the interface between (a-base metal) and (c-weld metal).

According to Nelson et al., when the crystalline structures of the weld metal and the base metal are different at freezing temperature, nucleation of solid weld metal occurs in heterogeneous locations at the fusion boundary on a semi-melted base metal. Therefore, as a result of heterogeneous nucleation at the boundary of the molten pool, the melting boundary would have non randomness orientations between the base metal and the weld metal

grains. Weld metal grains can follow the orientations of the base metal grains or not. That is, these grains can put themselves in such a way that their certain atomic plates placed parallel to the plates and special directions of the base metal grains [16]. In the samples that sub-layer of nickel is not used in them, due to the fact that the weld metal and the base metal both have the crystalline lattice of BCC also there is no limitation in terms of solubility at ambient temperature, new grains with following base metal grains have grown in form of cellular and plate (Fig. 6-A). However, in two samples that the nickel was used as a sub-layer, some of the nickel penetrates into the weld (Fig. 6-B). Since nickel has an FCC crystalline lattice and with the advancement of freezing and reaching the ambient temperature, solubility decreased. The dendritic growth of the grains occurs in the welding metal. Fig. 7 shows epitaxial growth and competitive growth in this alloy [16].

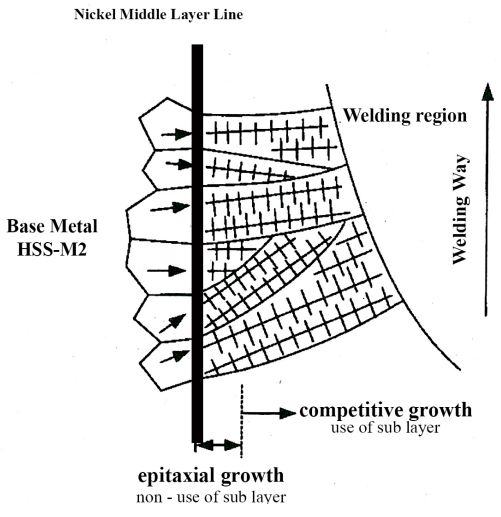

Fig. 7. Epitaxial and competitive growth in two modes of non- use and use sub-layer [16].

3. 2. Structural analysis

Fig. 8. Shows the XRD results of HM2-1, HM2-2, HM2-1Ni, HM2-2Ni samples. Except for the HM2 sample, which is the same as the raw material, the remaining samples (HM2-1-Ni and HM2-2-Ni and HM2-1 and HM2-2) have conformity in the W_2C, WC, Fe_3W_3C peaks that are indicated on the graph with the signs. Also, in samples HM2-1-Ni and HM2-2-Ni, nickel peak that is indicated with lozenge corresponded to each other and at the end; Fe in each of the five samples existed and corresponded with each other. In the HM2 sample, only one peak related to the Fe phase was observed, and in four other samples in addition to Fe, W_2C, WC, Fe_3W_3C phases were also observed. Lane et. al. obtained similar results [3], but Bechley et.al. achieved the microstructure of eutectic and M_7C_3 carbides is different to this study [4].

In most cases the formation of M_7C_3 carbides decreased wear resistance [1,3,4].

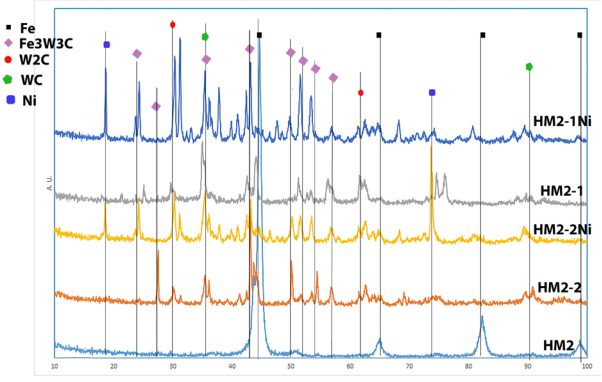

Fig. 8. XRD test results on HM2-1, HM2-2, HM2-1Ni, HM2-2Ni samples.

3. 3. Microhardness test

Fig. 9 shows the microhardness changes from the weld metal to the sub-layer and the base metal to a distance of 5 mm from the end of the weld metal. As it is seen, due to the presence of elements such as chrome, cobalt, and tungsten in the weld metal, the hardness number has increased. The closest area to the welding zone due to the dampening of existing martensites had a lower hardness than the metal base. It is also observed that samples cladded with that two-layer of tungsten carbide had the higher input temperature, in this situation, tempering has been done for a long time and the hardness reduced. The maximum hardness of the surface was about 2000 HV, which shown about 25 percent increase compared to the other research that used tungsten carbide powder coatings [2].

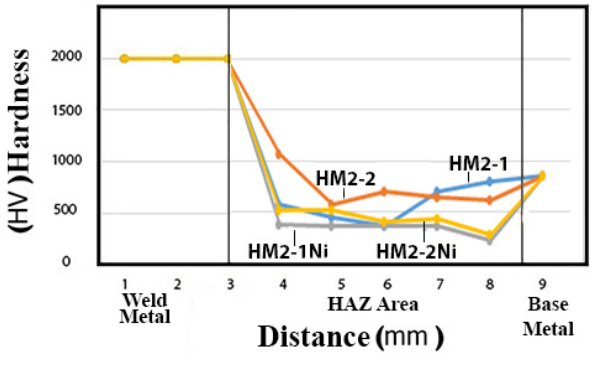

Fig. 9. Hardness profile from the surface of the coating.

3. 4. Wear test

The results of wear test according to ASTM G65 presented in Table 3. The lost volume of each sample is obtained, Fig. 10, shows the amount of lost volume of each sample in cubic millimeters.

As can be seen, the percentage of lost volume of weld metal compared to base metal is much lower and the wear resistance in the coating has improved to a satisfactory level. The most important reason for achieving these results is the presence of tungsten carbide in the weld metal, creating a ceramic compound and increasing hardness to more than 2000 HV. According to the results, it was observed that samples in which pure nickel was used as a sub-layer metal, led to dendrite freezing and coarse grains, wear resistance reduced and the volume by about 40% lost. Instead, the samples were used without using the sub-layer and with regard to the epitaxial growth of the weld metal grains and shrinking them; so that increase wear resistance and reduce loss of lost volume. In HM2-1 and HM2-2 samples, it is observed the uniform distribution of elements in the structure that tungsten carbide in the structure caused a uniform increase in wear resistance throughout the plot. On the other hand, in HM2-1-Ni and HM2-2-Ni samples, the rejection of the elements towards the grain boundary increased, which resulted in a reduction in wear resistance and an increase in the lost volume. So, all the reasons that caused changes in the metal structure, such as cooling rate and alloying elements, were directly related to wear resistance which must be considered to be improved.

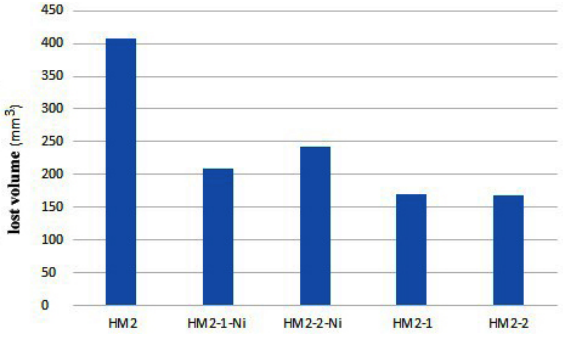

Fig. 10. The lost volume diagram in mm^3.

3. 5. Study of wear surfaces

Fig. 11 shows the wear surfaces of samples after wear test. Surface quality of the raw sample is better than two other samples, but due to less friction between them low contact surface with the disk accrued, so that there is more lost volume. Also, the surface of the wear test in the raw sample is much softer than the samples with Tungsten carbide coating. Also, the wear surface of the HM2-1 and HM2-2 samples changed less than the HM2-1-Ni and HM2-2-Ni samples, due to the formation of dendritic grains and the ununiformed hardness and wear resistance. these samples showed more roughness in the fracture surface. The presence of wear scratching is also visible in all samples.

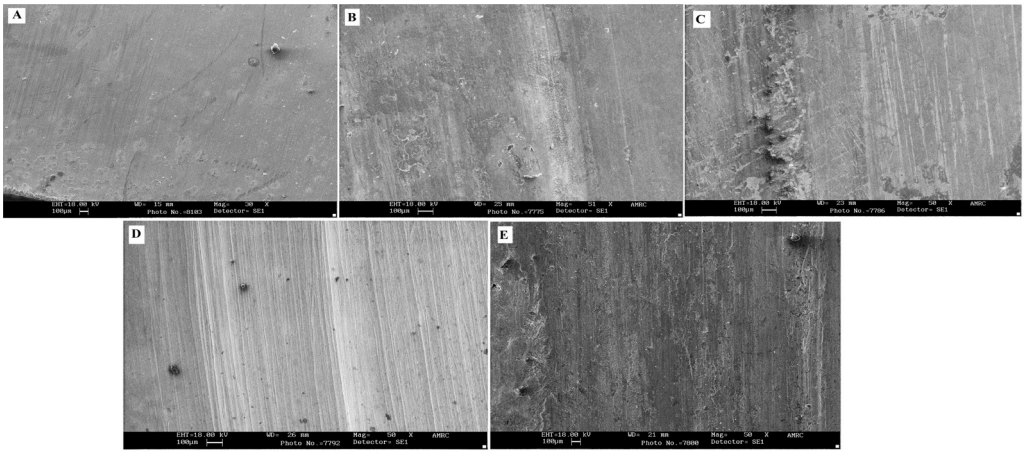

Fig. 11. Wear surface of samples A-HM2, B-HM2-1-Ni, C-HM2-2-Ni, D-HM2-1, E-HM2-2 After wear test ASTM G65.

4. Conclusion

- By using interlayer Nickel (with FCC crystalline lattice), grain has grown in the weld metal transfer from the epitaxial state to non-epitaxial.
- By applying the tungsten carbide layer, the hardness of the coated steel compared to the uncoated steel sample increased, which was due to the microstructural changes and the presence of hard particles in these coatings.
- By applying the nickel sub-layer and welding tungsten carbide on a raw sample, the lost volume in the wear test has decreased by 50%, also in conditions without the use of sub-layer of nickel and applying tungsten carbide on the raw material sample, the lost volume decreased by 60% in the wear test.
- In samples with sub layer of nickel, the growth of grains was a dendritic that caused a rise of 1.5 times of the lost volume than the non-applied samples in the wear test.
- By applying heat during welding to the surface of the work piece due to the annealing of the martensitic structure, the degree of hardness at the base metal was reduced about 50%, which increased the toughness of the parts.
- In the use of a coated and non-applied sub-layer of nickel, due to the higher concentration of tungsten carbide in the surface, there was less volume lost (1.3%) than one layer during wear test.

References

[1] M. Khadem, O. V. Penkov, H. K. Yang, D. E. Kim: Friction., 5(2017), 248.
[2] M.Riabkina-Fishman, E. Rabkin, P. Levin, N. Frage, M.P. Dariel, A. Weisheit, R. Galun, B.L. Mordike: Mater. Sci. Eng., 302(2001), 106.
[3] Y. C. Lin, K.Y, Chang, J. Mater. Process. Techn., 210(2010), 219.
[4] M. F. Buchely, J. C. Gutierrez, L. M. Leon, A. Toro: Wear., 259(2005), 52.
[5] S. F. Gnyusov, V. G. Durakov, S.Yu. Tarasov, Adv. Trib., 2012(2012), 1.
[6] S. W. Wang, Y. C. Lin, Y. Y. Tsai: J. Mater. Process. Techn., 140(2003), 682.
[7] M. Bonek: Arch. Mater. Sci. Eng., 58(2012), 182.
[8] C. Roda-Vazquez, A. Loureiro, J. P. Cribeiro: Mantenimiento, 134(2000), 78.
[9] G.B.Ottonello: Weld. Int., 21(2007), 569.
[10] N. Hashemi: Sur. Coat. Techn., 315(2017), 519.
[11] V. M. Fomin, AIP Conference Proc., (2016), 1770.
[12] J. Huebner, Arch. Metall. Mater. 62(2017), 531.
[13] ASTM G65, Standard Test Method for Measuring Abrasion Using the Dry Sand/Rubber Wheel Apparatus, Designation: G 65 – 00.
[14] ASTM 11-384" Standard Test Method for Knoop and Vickers Hardness of Materials" Book of Standards, Vol. 03,.01, 2011.
[15] Dantzig J. A., Chalmers M. R., B., Solidification, EPFL press, Swiss, 2016.
[16] Nelson, T., W., Lippold, J. C., and Mills, M. J., Weld. J., 78:329s, 1999.